快速热退火对 InGaAsSb/AlGaAsSb 多量子阱材料发光特性的影响

申琳，唐吉龙*，贾慧民**，王登魁，房丹，方铉，林逢源，魏志鹏

长春理工大学高功率半导体激光国家重点实验室，吉林 长春 130022

摘要 I 型 InGaAsSb/AlGaAsSb 量子阱是 1.8～3 μm 波段锑化物半导体激光器的首选材料，为进一步提升分子束外延生长的 InGaAsSb/AlGaAsSb 量子阱材料的光学性能，本文对其进行了快速热退火处理，通过光致发光光谱研究了快速热退火对量子阱材料光致发光特性的影响。光致发光光谱测试结果表明，快速热退火会使量子阱结构中垒层、阱层异质界面处的原子互扩散，改善量子阱材料的晶体质量，促使结构释放应力，进而提高了量子阱材料的光学性能。随着退火温度升高，量子阱材料的室温光致发光谱峰位逐渐蓝移，在 500,550,600 ℃ 退火后，量子阱材料光致发光谱的峰位分别蓝移了 7,8,9 meV。通过变温及变功率光致发光光谱测试，确认了样品发光峰的来源，位于 0.687 eV 的发光峰为局域载流子的复合，位于 0.701 eV 的发光峰为自由激子的复合。对不同退火温度的样品进一步研究后发现，退火温度的升高降低了材料中局域态载流子复合的比例，在 600 ℃ 退火温度下局域载流子与自由激子的强度比值降为 500 ℃ 退火温度下的 22.6%，这表明合适温度的快速热退火处理可以有效改善量子阱材料的光致发光特性。

关键词 光谱学；光致发光；InGaAsSb/AlGaAsSb；量子阱；快速热退火；局域态

中图分类号 O433.4；O472+.3　　　**文献标识码** A　　　　　　　　**doi**：10.3788/CJL202148.0711001

1 引　言

近年来，Ⅲ-Ⅴ 族半导体材料被广泛应用于激光器[1-2]、探测器[3-4]、发光二极管（LED）[5-6] 等光电子器件中。其中，InGaAsSb/AlGaAsSb 量子阱材料的禁带宽度在 GaSb 和 InAs 之间，是 1.8～3 μm 波段锑化物半导体激光器有源区[7-10] 的首选材料，引起了研究人员的广泛关注[11-14]。然而，对于锑化物合金半导体材料而言，在分子束外延（MBE）生长过程中会不可避免地引入一定的缺陷及分子团簇，导致材料局域态发光[15-17]，降低了材料的发光特性，从而最终影响了激光器的阈值电流、输出功率以及激光的线宽等。

为优化半导体材料的性能，研究人员通常对其进行退火热处理。1999 年，Xin 等[18] 对 GaInNAs/GaAs 多量子阱进行了快速热退火（RTA）处理，即在 650～850 ℃ 处理 10 s，结果发现，快速热退火处理后，多量子阱的光致发光（PL）强度增加，光谱发光峰位蓝移，多量子阱的界面形貌得到了改善。2000 年，Pan 等[19] 研究了 GaInNAs/GaAs 量子阱在 650 ℃ 处理 10 min 和在 900 ℃ 处理 5 s 后的光致发光特性，结果发现：650 ℃ 处理 10 min 的量子阱样品的光致发光强度较未处理样品增强了 50 倍，半峰全宽（$w_{1/2}$）无显著变化；900 ℃ 处理 5 s 后的量子阱样品的光致发光强度较未处理样品增强了 15 倍，半峰全宽减小了 11 meV，快速热退火处理后量子阱样品 PL 谱峰位发生了蓝移。2005 年，Kudrawiec 等[20] 对 GaNAsSb/GaAs 单量子阱材料进行了退火处理，退火量子阱样品的 PL 谱表明，其缺陷态发光强度降低，室温 PL 谱峰值强度增大了 10 倍，PL 峰位蓝移。2010 年，Kawazu 等[21] 分别在 675,700,725,750,800,825 ℃ 下对 GaSb Ⅱ 型量子

点进行了快速热退火处理,退火样品的 PL 谱显示,在 650～750 ℃进行快速热处理的样品的 PL 发光强度降低为热处理前的 1/10,而在 750～825 ℃进行快速热退火处理的样品的 PL 发光强度增强了三个数量级,且随着退火温度的升高,PL 峰位发生了蓝移。2012 年,Ulloa 等[22]在 850 ℃下对 InAs/GaAs II 型量子点进行了 30 s 的快速热处理,结果发现,与热处理前相比,样品的 PL 谱得到有效改善,15 K 时 PL 谱的峰值强度增加了 10 倍,半峰全宽减小了 65 meV,PL 谱峰位蓝移了约 149 meV。2014 年,Das 等[23]对 GaSbBi 薄膜进行了 500,550,600,650 ℃的退火处理,结果发现,退火后,位于 0.72 eV 的反位缺陷峰消失,随着退火温度升高,PL 谱的峰值逐渐增强而半峰全宽减小。

上述研究表明,对半导体材料进行快速热退火处理可以有效改善材料的质量,有利于外延晶体材料中残余应力的释放,改善合金材料的均匀性,减少晶体材料中的晶格缺陷。因此,合适的快速热退火是改善半导体材料质量的一种重要方法,已被广泛用于改善半导体发光材料的光电特性。目前,关于快速热退火对四元合金 InGaAsSb/AlGaAsSb 多量子阱材料发光特性影响的研究较少,因此,开展快速热退火处理对 InGaAsSb/AlGaAsSb 多量子阱材料发光机制影响的研究,对于实现 InGaAsSb/AlGaAsSb 量子阱激光器性能的进一步提高具有重要意义。

本文系统研究了快速热退火对 InGaAsSb/AlGaAsSb 多量子阱结构材料发光机制的影响。首先测试并对比了快速热退火处理前后量子阱材料的 PL 谱,然后对快速热退火处理前后量子阱材料的变温 PL 以及 10 K 时的变功率 PL 谱进行分析,以研究快速热退火处理对 InGaAsSb/AlGaAsSb 多量子阱材料发光特性的影响。

2 实 验

采用 DCA-P600 分子束外延系统,在 N 型 GaAs 衬底上生长厚度为 500 nm 的 GaSb 缓冲层,接着在缓冲层上生长三周期 $In_{0.1}Ga_{0.9}As_{0.08}Sb_{0.92}$/$Al_{0.3}Ga_{0.7}As_{0.13}Sb_{0.87}$ 量子阱结构,其中,$In_{0.1}Ga_{0.9}As_{0.08}Sb_{0.92}$ 阱层厚度为 20 nm,$Al_{0.3}Ga_{0.7}As_{0.13}Sb_{0.87}$ 垒层厚度为 30 nm。将生长的样品解理为大小相等的 4 块,其中一块作为对比样品,另外 3 块在氮气氛围下进行快速热退火处理,退火温度分别为 500,550,600 ℃,退火时间均为 30 s。

采用 655 nm 连续输出半导体激光器作为 PL 谱激发源,激光光斑面积为 0.4 cm²。利用带有 InGaAs 探测器的 HORIBA iHR550 光谱仪检测 PL 信号,探测器温度保持在 −30 ℃,光谱仪选择刻线密度为 600 line/mm 的光栅,选择波长为 1000 nm 的滤波片,所有测试均在带有 CaF₂ 窗口的封闭循环液氮低温冷台上进行。在变功率 PL 测试中,激光功率密度的变化范围为 1～300 mW/cm²;在变温 PL 测试中,温度的变化范围为 10～300 K。

3 实验结果与讨论

为研究快速热退火对 InGaAsSb/AlGaAsSb 量子阱材料发光性能的影响,对未处理样品以及在不同温度下进行快速热退火处理的样品进行室温 PL 谱测试,PL 峰位分别标记为 A、B、C 和 D,激发功率密度为 300 mW/cm²,结果如图 1 所示。为清晰地观察室温 PL 谱的峰位变化,对 PL 谱进行了归一化处理,从图 1 中可以看到未处理样品的室温 PL 谱发光峰(A)位于 0.632 eV,而在 500,550,600 ℃进行快速热退火的样品的室温 PL 谱发光峰(B、C 和 D)分别位于 0.639,0.640,0.641 eV。
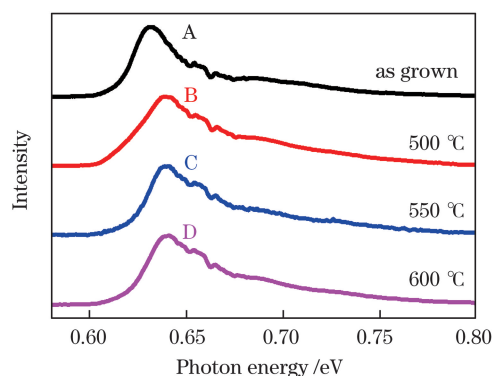

图 1 未处理样品以及分别在 500,550,600 ℃下退火 30 s 样品的室温 PL 谱

Fig. 1 Room temperature PL spectra of as-grown sample and samples annealed at 500 ℃, 550 ℃ and 600 ℃ for 30 s

由图 2 可以看出,退火样品的 PL 峰位相对未处理样品的 PL 峰位分别蓝移了 7,8,9 meV,退火样品的半峰全宽随着退火温度的升高呈先下降后升高的趋势。随着退火温度升高,量子阱中的 In 组分会析出形成团簇,随后团簇进一步扩散,从而影响了半峰全宽。随着退火温度升高,发射峰位发生了不同程度的蓝移,这与文献[24]中报道的相符。以上表明,快速热退火对量子阱材料的光致发光特性产生了影响。
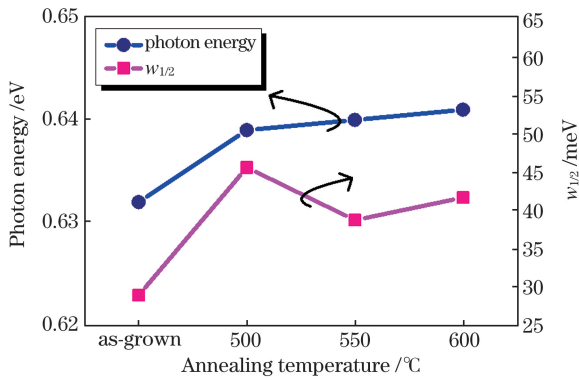
图 2　未处理样品以及退火样品的室温 PL 谱峰位和半峰全宽

Fig. 2　Peak position and full width at half maximum of room temperature PL spectra of as-grown sample and samples treated at different annealing temperatures

对于四元合金 InGaAsSb/AlGaAsSb 量子阱材料来说,快速热退火会引起异质界面元素的原子互扩散。如图 3 所示,这种原子互扩散分为两类[25]:1)Ⅲ族元素的原子互扩散,如 Al、In 和 Ga 原子在界面处扩散;2)Ⅴ族元素的原子互扩散,如 As 和 Sb原子在界面处扩散。这两种异质界面元素的原子互扩散使得 InGaAsSb/AlGaAsSb 量子阱的带隙增大,导致量子阱中的基态跃迁能量增加,从而使量子阱材料室温 PL 谱的峰值发生蓝移。

为了明确 InGaAsSb/AlGaAsSb 量子阱材料的室温发光机制,本文对未处理的 InGaAsSb/AlGaAsSb 量子阱样品在 10 K 条件下进行了变功率 PL 谱测试,测试结果如图 4 所示。图 4(a)为未处理样品在 10 K 温度下的变功率 PL 谱,激发功率密度范围为 1~300 mW/cm²(由下至上)。在低温
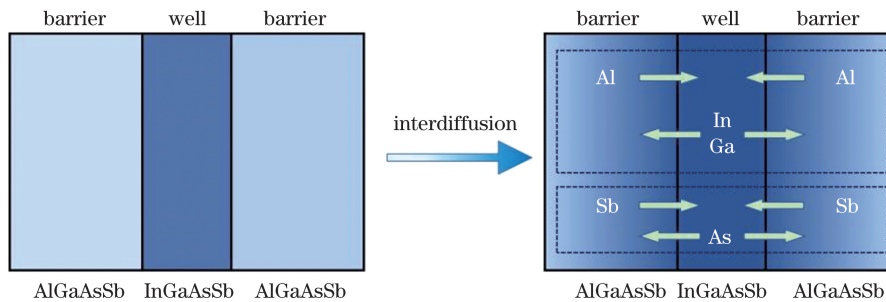

图 3　InGaAsSb/AlGaAsSb 量子阱材料中原子互扩散示意图

Fig. 3　Schematic of atomic interdiffusion in InGaAsSb/AlGaAsSb quantum well material
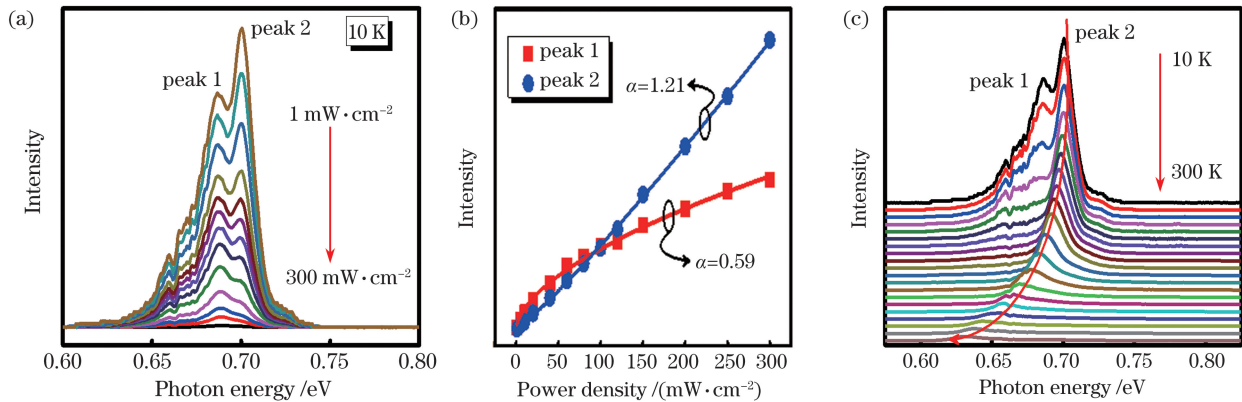

图 4　未处理量子阱样品的变功率 PL 谱和变温 PL 谱。(a)(b)变功率 PL 光谱及拟合曲线;(c)变温 PL 光谱

Fig. 4　Power-dependent and temperature-dependent PL spectra of as-grown quantum well sample.
(a)(b) Power-dependent PL spectra and fitting curve; (c) temperature-dependent PL spectra

PL 谱中可观察到 2 个发光来源,将光子能量较低的发光峰标记为 peak 1,将光子能量较高的发光峰标记为 peak 2,这两个发光峰峰位分别为 0.687 eV 和0.701 eV。当激发功率较低时,peak 1 占主导地位,随着激发功率增加,peak 2 发光明显增强并占据主导地位。

PL 谱的积分强度与激发功率之间存在着一定的关系[26],该关系通常用于确定半导体中的发光来源。该关系的表达式为

$$I = \eta I_0^\alpha, \qquad (1)$$

式中:I 为发光强度;I_0 为激光辐射功率;η 为辐射效率;指数 α 为判断辐射复合机制的常数。根据 α

的值可以对发光复合机制进行判断：当 1<α<2 时，发光来自激子复合；当 α≈2 时，发光来源于电子-空穴发光或双激子发光；当 α<1 时，为杂质或者缺陷的发光[27-28]。

用(1)式对量子阱材料的变功率 PL 谱进行拟合，拟合结果如图 4(b)所示，拟合得到的 peak 1 的 PL 积分强度随激发功率变化的 α 值为 0.59，peak 2 的 PL 积分强度随激发功率变化的 α 值为 1.21。由于 peak 1 的 α 值远小于 1，因此可以初步判断 peak 1 来自局域载流子的复合，peak 2 来自自由激子的复合。随着功率密度增加，局域态被载流子填充逐渐饱和，更多的光激发载流子占据带边的扩展态，所以带边发光逐渐增强。

为进一步确认样品发光机制的判断，对未处理量子阱样品进行了 10～300 K（由上至下）的变温 PL 谱测试，结果如图 4(c)所示。随着温度升高，peak 2 的光子能量逐渐减小，发射波长向长波方向移动，peak 1 在 50 K 时猝灭。peak 1 的猝灭是由于

当温度升高时，局域载流子获得了一定的热能，从局域态中逃出[29]，因此室温下的 PL 谱以 peak 2 发射为主。这一现象进一步证明了 peak 1 来自局域载流子复合以及 peak 2 来自自由激子复合的判定是正确的。

为探究快速热退火对量子阱样品发光特性的影响，本文对不同退火温度的量子阱样品进行了低温（T=10 K）PL 检测，并对检测结果进行了高斯拟合，结果发现使用 4 个高斯峰进行拟合的效果较好。图 5(a)为快速热退火处理量子阱样品的 PL 光谱及其拟合曲线，可以看出，随着退火温度升高，左侧低能端 peak 1 肩膀峰的发光降低，右侧高能端 peak 2 肩膀峰的发光增强。图 5(b)给出了 peak 1 和 peak 2 的发光强度，图 5(c)给出了强度之比，可以看到局域载流子发光占比逐渐减小，自由激子发光占比逐渐升高，600 ℃ 退火量子阱样品 peak 1 和 peak 2 的强度之比降为 500 ℃ 退火样品的 22.6%，此现象说明快速热退火有利于促进量子阱样品结构缺陷的愈合。

图 5　低温下 PL 光谱的拟合及发光强度。(a)不同退火温度下量子阱样品的 10 K 低温 PL 光谱及拟合曲线；(b) peak 1 和 peak 2 的发光强度；(c) peak 1 和 peak 2 的发光强度之比

Fig. 5　The fitting of PL spectra at low temperature and luminous intensity. (a) Low temperature (10 K) PL spectral and fitting curve of samples treated at different annealing temperatures; (b) luminous intensity of peak 1 and peak 2; (c) luminous intensity ratio of peak 1 to peak 2

从低温 PL 光谱可以看出，快速热退火对量子阱材料的光致发光机制具有一定影响。当快速热退火的温度升高时，量子阱材料的原子互扩散程度增加，互扩散消除了量子阱内部及界面处的缺陷，从而

提高了晶体的质量。对比不同退火温度下量子阱样品的低温 PL 谱可以看到，随着退火温度升高，局域载流子发光强度逐渐降低，自由激子发光强度逐渐增大。

对低温 PL 谱的拟合曲线进行分析可以发现，样品的发光峰位和半峰全宽与室温 PL 谱拟合曲线的变化趋势相同（如图 6 所示），即：随着退火温度升高，低温 PL 谱的发光峰位由于元素互扩散而出现蓝移，半峰全宽呈先减小后增加的现象。这是由于过高的温度导致量子阱层间组分发生偏析，形成了新的团簇。但是这些团簇并没有影响自由激子的发射，反而弥补了阱中的缺陷，使得局域态发光强度降低。以上现象说明快速退火引起的原子互扩散在提高晶体质量的同时提高了自由激子发光强度的比例，从而证明了快速热退火是提高量子阱发光效率的有效方法。
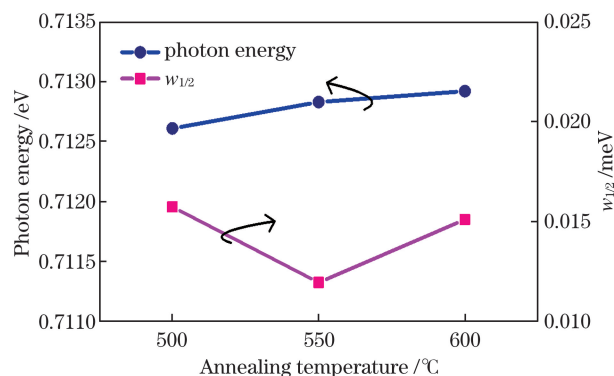

图 6 不同温度退火样品的低温 PL 谱峰位及半峰全宽

Fig. 6 Peak position and full width at half maximum of low temperature PL spectra of samples annealed at different temperatures

4 结 论

利用分子束外延系统，在 GaAs 衬底上生长了 InGaAsSb/AlGaAsSb 多量子阱结构，系统地研究了快速热退火对量子阱材料发光特性的影响。研究发现，快速热退火会使量子阱垒层、阱层异质界面的原子互扩散，从而使得量子阱材料的基态跃迁能量增加，导致量子阱样品的室温 PL 峰值发生蓝移。通过变功率 PL 谱和变温 PL 谱确定了量子阱样品的发光来源，低能端的发光峰为局域态载流子的复合，高能端的发光峰为自由激子的复合。快速热退火温度的升高降低了材料的局域载流子发射，说明快速热退火有利于使扩散产生的原子团簇均匀分布，也可以促使空穴愈合。这些结果表明，采用合适的温度进行快速热退火处理可以对激光器材料中的发光来源进行调控，进而有效提升激光器材料的发光性能，最终提高激光器的发光性能。

参 考 文 献

[1] Yuan Y, Chai X L, Yang C A, et al. 2.75-μm mid-infrared GaSb-based quantum well lasers with quinary alloy barrier[J]. Chinese Journal of Lasers, 2020, 47(7): 0701026.
袁野, 柴小力, 杨成奥, 等. 2.75 μm 中红外 GaSb 基五元化合物势垒量子阱激光器[J]. 中国激光, 2020, 47(7): 0701026.

[2] Lü Z R, Zhang Z K, Wang H, et al. Research progress on 1.3 μm semiconductor quantum-dot lasers[J]. Chinese Journal of Lasers, 2020, 47(7): 0701016.
吕尊仁, 张中恺, 王虹, 等. 1.3 μm 半导体量子点激光器的研究进展[J]. 中国激光, 2020, 47(7): 0701016.

[3] Amtout A, Raghavan S, Rotella P, et al. Theoretical modeling and experimental characterization of InAs/lnGaAs dots in a well detector[C]//The 16th Annual Meeting of the IEEE Lasers and Electro-Optics Society, 2003. LEOS 2003, October 27-28, 2003, Tucson, AZ, USA. New York: IEEE Press, 2003: 923-924.

[4] Zhang J, Itzler M A, Zbinden H, et al. Advances in InGaAs/InP single-photon detector systems for quantum communication [J]. Light: Science & Applications, 2015, 4(5): e286.

[5] Chao P F, Xu Y C, Liu C H, et al. Optimization and preparation of GaN-based LED chip electrode structure [J]. Laser & Optoelectronics Progress, 2020, 57(7): 072301.
晁鹏飞, 许英朝, 刘春辉, 等. GaN 基 LED 芯片电极结构的优化及制备[J]. 激光与光电子学进展, 2020, 57(7): 072301.

[6] Lin S Y, Tseng C C, Lin W H, et al. Room-temperature operation type-II GaSb/GaAs quantum-dot infrared light-emitting diode[J]. Applied Physics Letters, 2010, 96(12): 123503.

[7] Rattunde M, Mermelstein C, Schmitz J, et al. Comprehensive modeling of the electro-optical-thermal behavior of (AlGaIn)(AsSb)-based 2.0 μm diode lasers[J]. Applied Physics Letters, 2002, 80(22): 4085-4087.

[8] Lin C, Grau M, Dier O, et al. Low threshold room-temperature continuous-wave operation of 2.24-3.04 μm GaInAsSb/AlGaAsSb quantum-well lasers [J]. Applied Physics Letters, 2004, 84(25): 5088-5090.

[9] Kim J G, Shterengas L, Martinelli R U, et al. High-

power room-temperature continuous wave operation of 2.7 and 2.8 μm In(Al)GaAsSb/GaSb diode lasers [J]. Applied Physics Letters, 2003, 83(10): 1926-1928.

[10] Wang C A, Shiau D A, Calawa D R. Growth and characterization of InAsSb/GaInAsAb/AlGaAsAb/GaSb heterostructures for wafer-bonded thermophotovoltaic devices [J]. Journal of Crystal Growth, 2004, 261(2/3): 372-378.

[11] Bründermann E. Widely tunable far-infrared hot-hole semiconductor lasers [M]//Long-Wavelength Infrared Semiconductor Lasers. Hoboken, NJ, USA: John Wiley & Sons, Inc., 2005: 279-350.

[12] Choi H K, Walpole J N, Turner G W, et al. GaInAsSb-AlGaAsSb tapered lasers emitting at 2.05 μm with 0.6-W diffraction-limited power [J]. IEEE Photonics Technology Letters, 1998, 10(7): 938-940.

[13] Garbuzov D Z, Lee H, Khalfin V, et al. 2.3–2.7-μm room temperature CW operation of InGaAsSb-AlGaAsSb broad waveguide SCH-QW diode lasers [J]. IEEE Photonics Technology Letters, 1999, 11(7): 794-796.

[14] Li W, Heroux J B, Shao H, et al. High-T_0 strain-compensated InGaAsSb-AlGaAsSb quantum-well lasers emitting at 2.43 μm [J]. IEEE Photonics Technology Letters, 2005, 17(3): 531-533.

[15] Gao X, Wei Z, Zhao F, et al. Investigation of localized states in GaAsSb epilayers grown by molecular beam epitaxy [J]. Scientific Reports, 2016, 6: 29112.

[16] Baranowski M, Syperek M, Kudrawiec R, et al. Carrier dynamics between delocalized and localized states in type-II GaAsSb/GaAs quantum wells [J]. Applied Physics Letters, 2011, 98(6): 061910.

[17] Baranowski M, Syperek M, Kudrawiec R, et al. Carrier dynamics in type-II GaAsSb/GaAs quantum wells [J]. Journal of Physics: Condensed Matter, 2012, 24(18): 185801.

[18] Xin H P, Kavanagh K L, Kondow M, et al. Effects of rapid thermal annealing on GaInNAs/GaAs multiple quantum wells [J]. Journal of Crystal Growth, 1999, 201/202: 419-422.

[19] Pan Z, Li L H, Zhang W, et al. Effect of rapid thermal annealing on GaInNAs/GaAs quantum wells grown by plasma-assisted molecular-beam epitaxy [J]. Applied Physics Letters, 2000, 77(9): 1280-1282.

[20] Kudrawiec R, Motyka M, Misiewicz J, et al. Photoluminescence from as-grown and annealed GaN$_{0.027}$As$_{0.863}$Sb$_{0.11}$/GaAs single quantum wells [J]. Journal of Applied Physics, 2005, 98(6): 063527.

[21] Kawazu T, Sakaki H. Effects of Sb/As intermixing on optical properties of GaSb type-II quantum dots in GaAs grown by droplet epitaxy [J]. Applied Physics Letters, 2010, 97(26): 261906.

[22] Ulloa J M, Llorens J M, Alén B, et al. High efficient luminescence in type-II GaAsSb-capped InAs quantum dots upon annealing [J]. Applied Physics Letters, 2012, 101(25): 253112.

[23] Das S K, Das T D, Dhar S. Effect of post-growth anneal on the photoluminescence properties of GaSbBi [J]. Semiconductor Science and Technology, 2014, 29(1): 015003.

[24] Bugge R, Fimland B O. Annealing effects in InGaAsSb quantum wells with pentenary AlInGaAsSb barriers [J]. Physica Scripta, 2006, T126: 15-20.

[25] Wang Y, Djie H S, Ooi B S. Interdiffusionin InGaAsSb/AlGaAsSb quantum wells [J]. Journal of Applied Physics, 2005, 98(7): 073508.

[26] Bergman L, Chen X B, Morrison J L, et al. Photoluminescence dynamics in ensembles of wide-band-gap nanocrystallites and powders [J]. Journal of Applied Physics, 2004, 96(1): 675-682.

[27] Cooper D E, Bajaj J, Newman P R. Photoluminescence spectroscopy of excitons for evaluation of high-quality CdTe crystals [J]. Journal of Crystal Growth, 1988, 86(1/2/3/4): 544-551.

[28] Schmidt T, Lischka K, Zulehner W. Excitation-power dependence of the near-band-edge photoluminescence of semiconductors [J]. Physical Review B, 1992, 45(16): 8989.

[29] Gao X, Wei Z P, Fang X, et al. Effect of rapid thermal annealing on the optical properties of GaAsSb alloys [J]. Optical Materials Express, 2017, 7(6): 1971-1979.

Effect of Rapid Thermal Annealing on Luminescence Properties of InGaAsSb/AlGaAsSb Multiple Quantum Wells Material

Shen Lin, Tang Jilong*, Jia Huimin**, Wang Dengkui, Fang Dan, Fang Xuan,
Lin Fengyuan, Wei Zhipeng

State Key Laboratory of High Power Semiconductor Laser, Changchun University of Science and Technology,
Changchun, Jilin 130022, China

Abstract

Objective　In recent years, III-V semiconductor materials have been widely used in optoelectronic devices, such as lasers, detectors, and LEDs, and have attracted widespread attention of researchers. Among these materials, the band gap of the InGaAsSb/AlGaAsSb quantum well structure is between that of GaSb and InAs. Therefore, the InGaAsSb/AlGaAsSb quantum well structure is the preferred material for the preparation of antimonide semiconductor lasers with a wavelength range of $1.8-3\ \mu$m. In molecular beam epitaxial (MBE) growth of antimony alloy semiconductor materials, defects and molecular clusters are introduced. These defects reduce the light-emitting characteristics of the materials, affecting the threshold current, output power, and spectral line width of the laser. In order to further improve the optical properties of InGaAsSb/AlGaAsSb quantum well materials, a rapid thermal annealing method is used to treat the quantum well structure. The effects of rapid thermal annealing on the performance of quantum wells are studied here using photoluminescence spectroscopy.

Methods　An InGaAsSb/AlGaAsSb quantum well structure is grown using a DCA-P600 MBE system. A GaSb buffer layer with a thickness of 500 nm is first grown on an n-type GaAs substrate. Then, three periods of $In_{0.1}Ga_{0.9}As_{0.08}Sb_{0.92}/Al_{0.3}Ga_{0.7}As_{0.13}Sb_{0.87}$ are grown on the buffer layer. The thickness of the $In_{0.1}Ga_{0.9}As_{0.08}Sb_{0.92}$ well layer is 20 nm and the thickness of the $Al_{0.3}Ga_{0.7}As_{0.13}Sb_{0.87}$ barrier layer is 30 nm. The as-grown sample is cleaved into four pieces of equal size. One of the samples is designated as the as-grown sample and does not undergo rapid thermal annealing. The other three samples are subjected to rapid thermal annealing for 30 s in a nitrogen atmosphere at either 500 ℃, 550 ℃, or 600 ℃. A laser with a wavelength of 655 nm and spot area of $0.4\ cm^2$ is used to measure the photoluminescence spectrum of the samples. A HORIBA iHR550 spectrometer, with an InGaAs detector kept at -30 ℃, is used to detect photoluminescence signals. The line density of the selected spectrometer grating is 600 line/mm and the wavelength of filter is selected 1000 nm. All tests are carried out in a closed-circulation liquid helium cryostat with a CaF_2 window. The laser power density is changed from $1\ mW/cm^2$ to $300\ mW/cm^2$ during the power-dependent photoluminescence measurement and the temperature is changed from 10 K to 300 K during the temperature-dependent photoluminescence measurement.

Results and Discussions　The photoluminescence results show that rapid thermal annealing causes atoms to interdiffuse throughout the quantum well layer and the barrier layer interface in the quantum well structure. This can improve the crystal quality of the quantum well material and reduce structural strain, thereby improving the optical properties of the quantum well material. At room temperature, the photoluminescence spectrum shows a gradual blue-shift with increasing annealing temperature. When the annealing temperature is 500 ℃, 550 ℃, and 600 ℃, the photoluminescence shift is 7 meV, 8 meV, and 9 meV, respectively (Fig. 2). From the temperature-dependent and power-dependent photoluminescence spectra, it can be seen that the emission peak at 0.687 eV is the result of local carrier recombination and the emission peak at 0.701 eV is the result of free exciton recombination (Fig. 4). The experimental results show that increasing the annealing temperature can reduce the proportion of local carrier recombination. When the temperature is 600°C, the intensity ratio of local carriers to free excitons is reduced to 22.6% of that of the sample annealed at 500 ℃ (Fig. 5). The experimental results show that the photoluminescence performance of the quantum well material can be effectively improved with the appropriate rapid thermal annealing temperature.

Conclusions　An InGaAsSb/AlGaAsSb quantum well structure was grown on a GaAs substrate using a MBE system and the effects of rapid thermal annealing on luminescence properties of the quantum well material are systematically discussed. The experimental results show that rapid thermal annealing causes interdiffusion of elements on the

heterogeneous interface between the quantum barrier layer and the well layer. This interdiffusion increases the energy of the ground state transition of the quantum well material and thus causes a blue-shift of the room temperature photoluminescence peak of the quantum well material. The emission of the quantum well samples is determined by excitation power-dependent photoluminescence spectrum and temperature-dependent photoluminescence spectrum. There is recombination of localized state carriers and recombination of free excitons at the low energy and high energy end of the photoluminescence peak, respectively. The localized carrier emission of the material is reduced with the increase of rapid thermal annealing temperature. These results show that rapid thermal annealing is beneficial for uniform distribution of atomic clusters produced by diffusion and that it can also promote healing of resulting holes. The rapid thermal annealing process can optimize emission in the quantum well structure when the appropriate annealing temperature is selected, thereby effectively improving the performance of laser materials and laser devices.